JOURNAL OF MATERIALS SCIENCE 14 (1979) 1095–1102

Phenomenology of fracture in hot-pressed silicon nitride

R. K. GOVILA, K. R. KINSMAN*, P. BEARDMORE
Research Staff, Ford Motor Company, Dearborn, Michigan 48121, USA

Fracture phenomenology in hot-pressed silicon nitride has been studied fractographically as a function of flaw size, temperature and loading rate. Surface cracks of controlled size were introduced using the microhardness indentation technique. At room temperature, the fracture stress was found to depend on initial crack size according to the Griffith relationship and extrapolation of the data indicated that inherent processing flaws of the order of 12 to 24 μm are strength-controlling in virgin material. Using a simplified Griffith approach, the fracture surface energy, γ, at 20° C for hot-pressed Si_3N_4 is about 22 000 erg cm^{-2}. Two mechanistic regimes were manifest in the temperature dependence of the fracture stress. A mixed mode of fracture consisting of transcrystalline and intergranular crack propagation occurred up to 1100° C; at 1200° C and above, subcritical crack growth (SCG) occurred intergranularly and the extent of SCG increased with increasing temperature. Similarly, the extent of SCG decreased with increasing loading rate.

1. Introduction

Polycrystalline silicon nitride, consolidated by hot-pressing, has received considerable attention as a ceramic material for structural applications primarily because of good oxidation resistance, low coefficient of thermal expansion, and retention of high strength up to 1000° C. Like many other ceramics, silicon nitride has little tolerance for incipient flaws which are present due to processing and fabrication. It is these random flaws which control the mechanical properties. Although several investigations [1–11] of the temperature-dependent mechanical properties are on record, few have addressed the mechanistic aspects of the fracture process except by inference. In this paper, we report the results of a series of simple mechanical tests performed on precracked specimens to measure the strength of hot-pressed Si_3N_4 (Norton HS-130 material) as a function of flaw size, temperature and loading rate. In addition, an estimate of the strength controlling flaws (or the inherent flaw size) of the as-received material, and the true fracture energy, γ, the onset of subcritical crack growth and subsequent crack propagation have been determined. Fractography is the principal interpretive agent for the presence of subcritical crack growth, and from which an appreciation for the vagaries of the mechanistic aspects can be drawn.

2. Experimental techniques

2.1. Sample preparation and testing

The material used in this study was a nominally fully dense, hot-pressed silicon nitride commercially known as HS-130†. While the nominal structure of hot-pressed Si_3N_4 is yet the subject of some discussion [12, 13], for the purpose of this investigation it may be considered to be comprised of a mixture of α- and β-Si_3N_4, and that the strength-limiting impurities segregate to the crystalline boundaries in the form of a less refractory phase. Interpretation [2, 5–9, 14] to date considers that the grain-boundary phase is a viscous glass at high temperatures, probably predominately unstable, comprised chemically of a combination of pro-

*Present address: Electric Power Research Institute, Palo Alto, California 94304, USA.
†Norton Company, Worcester, Mass., USA.

cessing aids, principally MgO and CaO, as well as SiO_2 residual to the Si_3N_4 powder used in fabrication.

Test specimens of dimensions 1 in. (~25 mm) long × ¼ in. (~6 mm) wide × ⅛ in. (~3 mm) thick were machined from blocks of material such that the tensile face was perpendicular to the hot-pressing direction (strong direction). All faces were ground in a lengthwise direction using 220-grit diamond wheels and the edges chamfered to prevent notch effects. One surface (the tension face in bending) was carefully ground and wet polished to 6 μm diamond finish. The specimens were then precracked using the indentation technique as outlined briefly in Section 2.2, and tested in four-point bending in an Instron testing machine at a constant cross-head speed of 0.005 in. min^{-1} (~0.127 mm min^{-1}). The outer and inner loading edges of the silicon carbide testing fixture were spaced 0.6 in. (~15 mm) and 0.2 in. (~5 mm) apart, respectively. High temperature (200 to 1450° C) bend tests were performed in air in a cylindrical muffle-furnace (Centorr Associates). In high temperature tests, specimens were held at the test temperature for about 15 min in order to achieve equilibrium before testing is started. No preload was applied on test specimens either at room temperature or at high temperature tests. Fracture surfaces were examined by optical microscopy and scanning electron microscopy (SEM).

2.2. Controlled precracking of specimens

Indenting this material with a Vickers diamond pyramid indenter resulted in the introduction of surface cracks of reproducible geometry and size controlled by choice of indenter load. This technique has been used successfully both in single

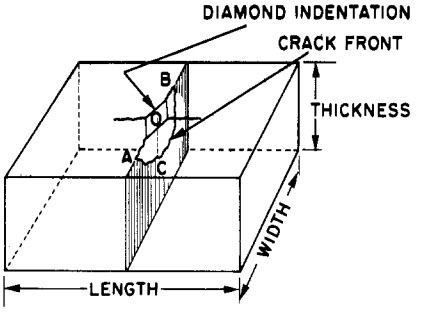

AB–Single Crack Produced by Diamond Indentation
ACB–Crack Front Produced by Indentation
(a) CO–Depth of Crack as Seen on the Fracture Plane

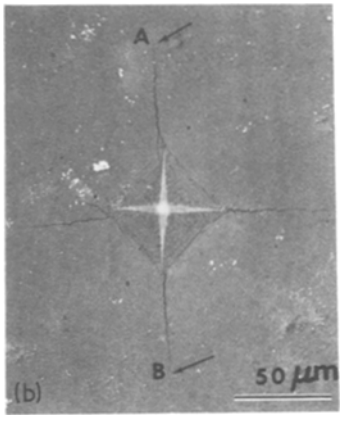

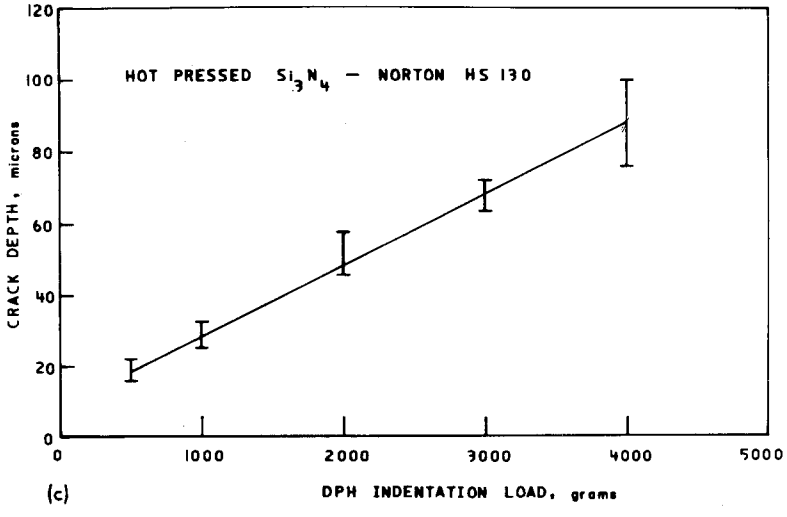

Figure 1 (a) Schematic representation of crack geometry as produced by microhardness indentation. (b) Typical crack produced on the polished surface of a hot-pressed silicon nitride HS-130 test specimen with 4000 g indentation load. (c) Crack depth (CO, as measured from the fracture faces of test specimens) as a function of indentation load.

crystals of vanadium carbide [15] and in polycrystalline materials [10, 11, 16–18]. The resultant crack geometry and the corresponding crack depths as measured from the fracture faces are shown in Fig. 1a and c, respectively. Typical example of a crack produced on the polished surface of a test specimen is shown in Fig. 1b. All indentations were made at room temperature.

3. Results and discussion

3.1. Fracture energy and inherent flaw size determination

The variation of fracture stress with crack depth for hot-pressed Si_3N_4 specimens tested at room temperature is shown in Fig. 2, and the data show a linear variation consistent with the Griffith [19] criterion for brittle fracture:

$$\sigma_F \approx Y\left[\frac{E\gamma}{c}\right]^{1/2}, \qquad (1)$$

where σ_F is the fracture stress required to propagate a pre-existing crack of known dimensions, Y is a constant relating primarily to crack geometry and specimen dimensions, E is Young's modulus, c is the initial crack depth at which fracture initiated, and γ is the fracture energy. For approximately semi-circular cracks, Y is taken as unity [20]. Using a value of $E \approx 313.6 \times 10^{10}$ dyne cm^{-2} at 20° C as determined by ultrasonic measurement [21] for hot-pressed Si_3N_4 (HS-130) and the slope of the curve shown in Fig. 2, the computed value of fracture energy, γ, is $\sim 22\,000$ erg cm^{-2}. This low value of γ suggests that fracture occurs at 20° C in an essentially brittle manner involving little or no plasticity. It is important to note that the above can be taken rigorously only as a demonstration of principle. A body of evidence is accumulating which suggests that crack opening residual stresses can accompany hardness indentation induced cracks in similar materials [10, 16, 17, 22, 23]. Although our own studies [24] do not support the removal of residual stresses by annealing in air or vacuum in similar materials, the presence of such stress could significantly influence the absolute magnitude of the experimentally determined fracture energy.

Several authors [3, 4, 8, 25] have made measurements of fracture energy, γ, in hot-pressed Si_3N_4 using various techniques. Earlier estimates of γ by Coppala *et al.* [3] using the work of fracture method and Lange [4] using the double cantilever beam method resulted in considerably higher values of γ than the value determined in this study, possibly due to differences in microstructure and accompanying plastic deformation, respectively. Petrovic and Jacobson [25] using a similar method to the one used in this study found the value of $\gamma \approx 23\,000$ erg cm^{-2} for HS-130. Recently, Hartline *et al.* [8], using the work of fracture method, reported the γ value for HS-130 Si_3N_4 material to be about 25 000 erg cm^{-2} at 1000° C and further showed that γ increased with increasing temperature. It is assumed that γ remained constant from 20 to 1000° C because of essentially constant σ_F (see later). In view of the above discussion, it is considered that the value of $\gamma \simeq 22\,000$ erg cm^{-2} is a reasonable estimate of the fracture surface energy for hot-pressed Si_3N_4 (HS-130).

From a practical point of view, perhaps the most useful application of the data shown in Fig. 2

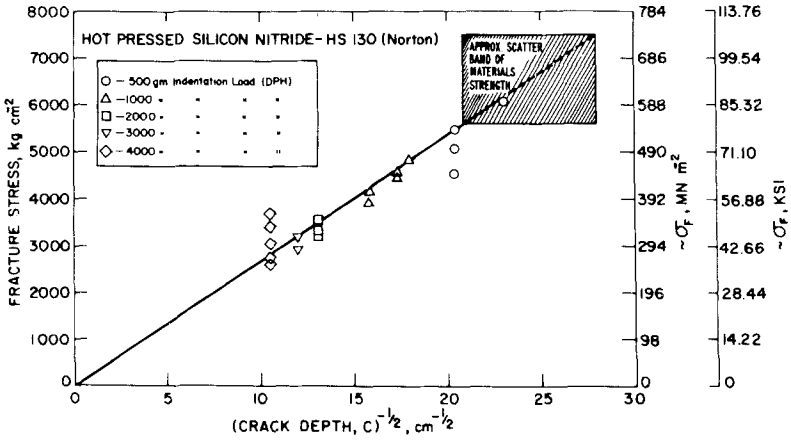

Figure 2 Variation of fracture stress as a function of inverse square root of crack depth at room temperature.

is as a means of estimating the inherent flaw size in hot-pressed Si_3N_4. Extrapolation of the data in Fig. 2 to the fracture stress of uncracked samples (shown as the approximate scatter band of materials strength) indicates that flaws of the order of 12 to 24 μm in depth are present in the as-received (uncracked) Si_3N_4. To date, this is perhaps the best estimate of the inherent flaw size in hot-pressed Si_3N_4 (HS-130). Lange [4] also estimated the flaw size to be around 90 μm in a similar type material from his surface energy measurements. This flaw size is too large to be realistic, since flaws of this magnitude should be readily identifiable by optical metallography.

3.2. Effect of temperature and subcritical crack growth

The temperature dependence of the fracture stress, σ_F, for uncracked (virgin) material and for precracked specimens (containing cracks of about 90 μm depth), and tested at temperatures between 20 and 1400° C is shown in Fig. 3. It is clear that σ_F for precracked specimens remains essentially constant and independent of temperature from 20 to 1100° C. The constancy of σ_F suggests that no change in fracture mechanism occurs and indicates little or no blunting of the crack tip by plastic deformation in this temperature region. A typical fracture surface of a specimen tested at 1000° C is shown in Fig. 4. Note that the mode of fracture in the precracked region (inside ACB), Fig. 4a, and in the repropagated region (outside ACB), Fig. 4b, is similar, i.e. a mixed mode of fracture consisting of transgranular and intergranular crack growth.

A rapid increase in σ_F occurs above 1100° C, leading to a maximum occurring between 1200 and 1250° C. This sudden increase in σ_F leading to a peak value indicates that the initial crack finds it more difficult to propagate as the temperature is raised. Since the crack path is confined to the grain boundary, the plasticity process at play is probably not a classical crack tip blunting in the sense that crystal dislocation slip accommodation occurs as is usually the case in single crystal studies [15]. Rather a displacement and general disruption of the continuity of the crack tip out of the emplaced crack due to viscous flow (softening of glassy phases) at the grain boundary is a more likely mechanism of "crack blunting". Up to 1200° C, the fracture surface appearance was similar to the lower temperature fractures (Fig. 4), and did not show any detectable presence of slow crack growth. Failure of precracked specimens occurred in a brittle (catastrophic) manner.

In general, subcritical (slow crack growth (SCG) or delayed fracture) refers to crack growth below the normal stress required to cause catastrophic failure of the specimen and the crack grows in a controlled manner such that the growth can be arrested by unloading the specimen at some stage of deformation. Using the stress rate approach [26] and the double torsion technique [27], indirect evidence for SCG in HS 130 Si_3N_4 has been presented earlier by Lange [7] and others [9, 28], respectively. However, the most convincing evidence of this phenomenon is by direct, controlled metallographic studies. Such data were developed in the present work by subjecting a precracked specimen containing an initial crack, AB $\approx$ 174 μm (Fig. 5), to a stress below the normal fracture stress at 1300° C, and the stress was allowed to relax for a short time (<2 min). The specimen was unloaded and examination of the tensile surface revealed that the original crack

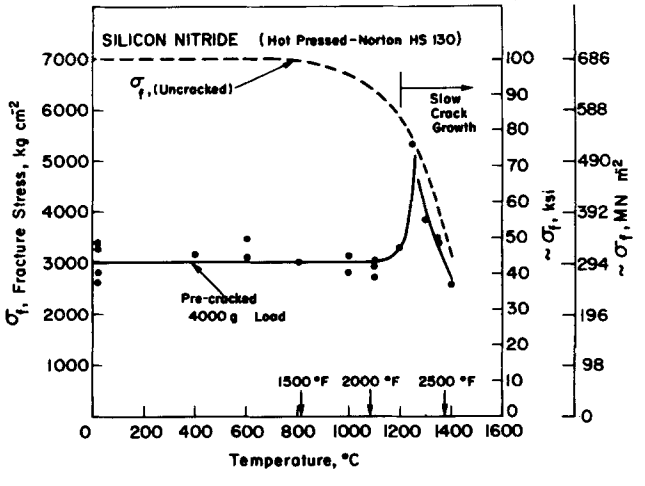

Figure 3 Effect of temperature on the fracture stress of uncracked and precracked (with 4000 g load indentation producing cracks of about 90 μm depth) specimens.

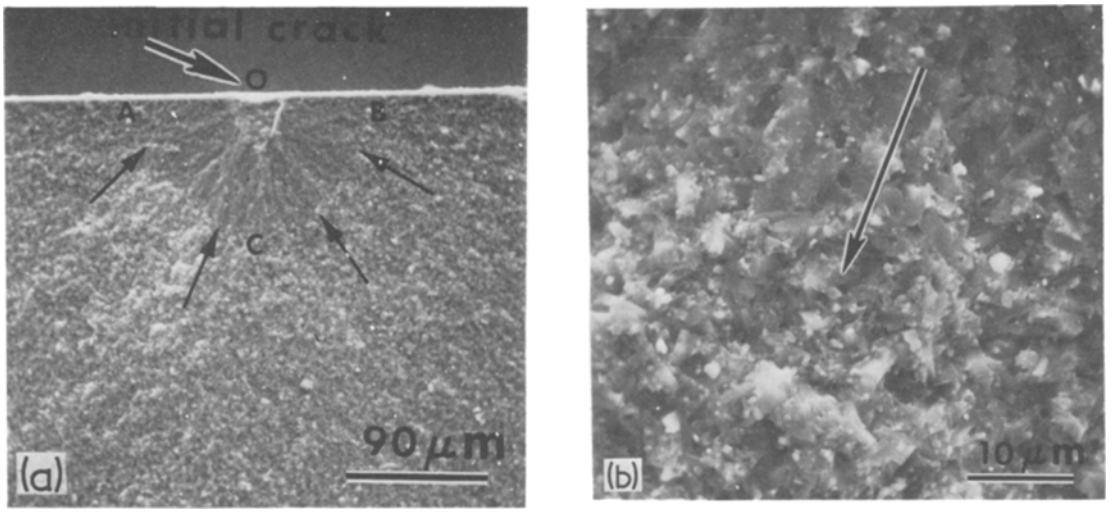

Figure 4 Typical SEM micrographs of fracture surface of a precracked (~ 90 μm deep) specimen of HS-130 Si_3N_4 tested at 1000° C in air. (a) ACB is the precracked region, (b) higher magnification view in the vicinity of region C. Arrow indicates the direction of crack propagation from precracked area to repropagated region.

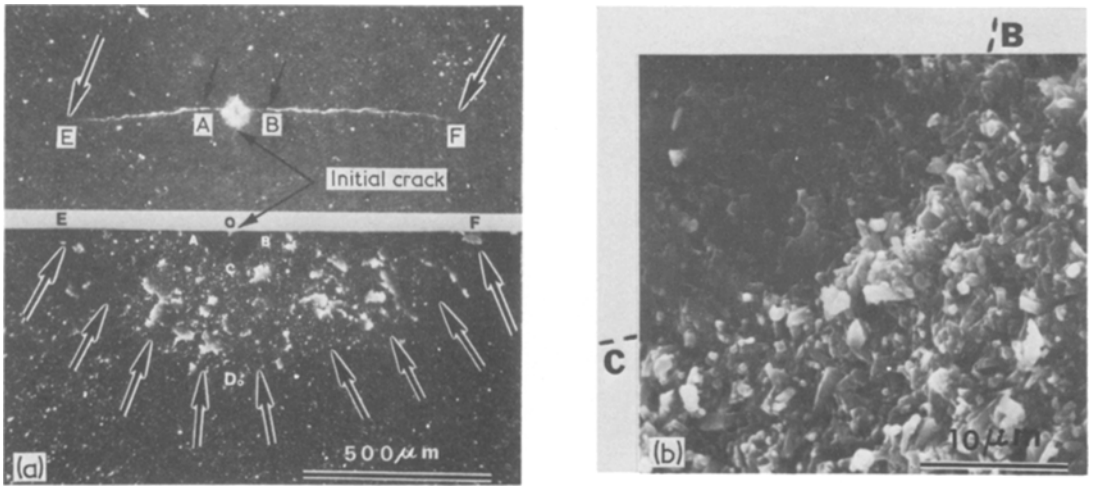

Figure 5 Metallographic evidence for the presence of subcritical crack growth (SCG) at 1300° C (a) specimen was precracked with 4000 g load indentation, producing a surface crack AB ≈ 174 μm (top photo) and about 85 μm deep and was stress relaxed for a short period at 1300° C to just below its normal fracture stress. Specimen was unloaded and micrograph of the tensile surface showed that the initial crack AB had grown to new length EF ≈ 1000 μm. Specimen was finally broken at 20° C and the fracture surface showed that the initial crack ACB had grown to EDF, matching with the surface length EF. Pictures taken with plane polarized light. (b) SEM view taken along the crack front boundary BC, revealing the nature of crack propagation during fast fracture (inside ACB) and subsequent slow crack growth (outside ACB).

AB had extended to length EF ≈ 1000 μm. The specimen was retested to failure at room temperature to determine if the fracture surface shows a one-to-one correlation between the extent of SCG and the extended length of the crack as seen on the tensile surface of the test specimen. Such evidence is clearly shown in Fig. 5a, where EDF is the boundary of the SCG region. The nature of the mode of crack propagation during the initial microcrack introduction (fast crack propagation) and subsequent SCG is shown in Fig. 5b.

The fracture surface appearance at 1200° C (Fig. 6a), is similar to that observed at lower temperatures (Fig. 4), and does not show the presence of SCG. The first signs of SCG of the initial microcrack were observed on the fracture face in tests made at 1250° C and higher temperatures (Fig. 6b) (as indicated by the change in reflectivity). The extent of SCG prior to catastrophic failure increased with increasing tempera-

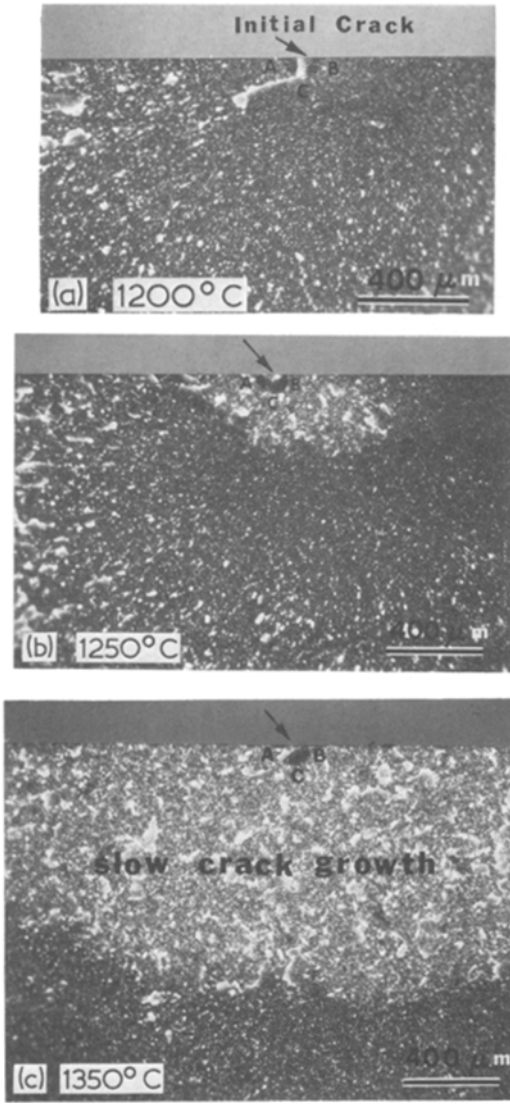

Figure 6 Typical fracture surfaces of precracked (crack depth $\approx 90\,\mu m$) HS-130 Si_3N_4 specimens tested at a machine head speed of 0.005 in. min^{-1} at various temperatures. Pictures taken with plane polarized light. Note the absence of subcritical crack growth (SCG) at 1200° C and subsequent appearance of SCG surrounding the initial crack at 1250° C and higher temperatures.

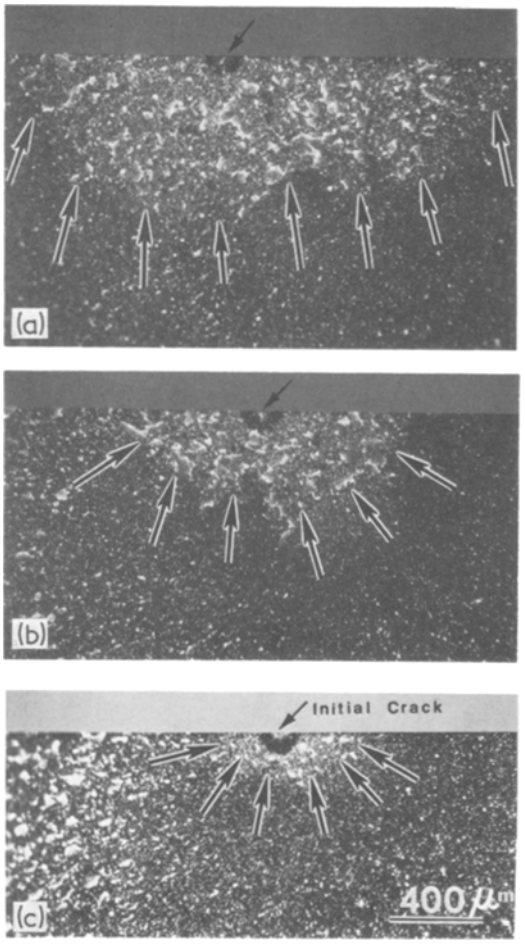

Figure 7 Successive stages in the subcritical crack growth of precracked specimens tested at 1300° C as a function of machine head speed. (a) MHS = 0.005 in. min^{-1}; (b) MHS = 0.05 in. min^{-1}; (c) MHS = 0.2 in. min^{-1}. All specimens contained cracks of about 90 μm depth. Pictures taken with plane polarized light.

ture (cf. Fig. 6b and c). The slow crack growth region is distinct in its appearance, characterized by bright whitish regions. The mode of fracture during SCG is completely intergranular Fig. 5b, but with significant excursions out of the mean fracture plane so that the optical reflectivity of the specimen is altered as apparent in the sequence (Fig. 6a to c). Above 1250° C, σ_F decreases abruptly (Fig. 3), with a proportional increase in SCG region. The two curves (Fig. 3), seem to merge and show a decreasing strength above 1250° C. The temperature at which the two curves merge characterizes the importance of SCG and points out that failure is governed by the extent of SCG and not by initial crack size. Precracked specimens which displayed large SCG also failed in a brittle (or catastrophic) manner in the sense that a sudden and sharp load drop occurred at the instant of failure and the load–deflection curve did not show significant deviation from the elastic line. Note that the initial cracks are close to a semicircular shape while the SCG region adopts a pseudo-elliptical shape.

3.3. Strain-rate dependence

The strain-rate sensitivity of SCG was determined in specimens containing a constant crack size (about 90 μm deep) and tested at a constant

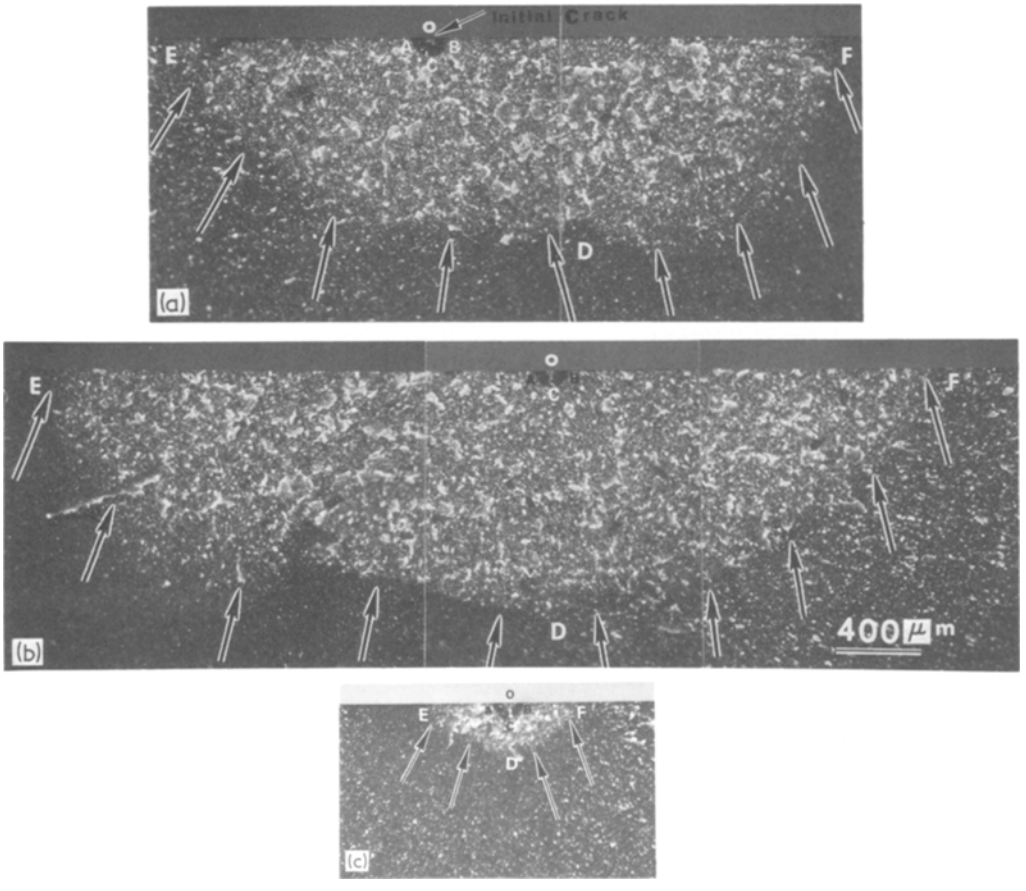

Figure 8 Successive stages in the movement of slow crack growth region of specimens tested at varying stress levels at 1300° C. All specimens contained cracks of about 90 μm depth. The symbol $\sigma_{A\text{-}C}$ stands for the applied stress that was kept constant and the symbol σ_F 1300° C stands for the average value of fracture stress at 1300° C for specimens precracked with 4000 g load indentation. Micrographs taken with plane polarized light and equal magnification. (a) Specimen loaded to a stress level, $\sigma_{A\text{-}C} \approx 0.90\,\sigma_F$ 1300° C, failed after 0.5 min. (b) Specimen loaded to a stress level, $\sigma_{A\text{-}C} \approx 0.73\,\sigma_F$ 1300° C, failed after 1.4 min. (c) Specimen loaded to a stress level, $\sigma_{A\text{-}C} \approx 0.62\,\sigma_F$ 1300° C, unloaded after 40 min, and finally broken at 20° C to reveal the extent of slow crack growth.

temperature of 1300° C (Fig. 7). Increasing the strain-rate (or the machine head speed) makes the material more brittle and initially raises the fracture stress. In agreement with this view, the extent (or depth) of SCG decreased as the strain-rate increased until it disappeared at a machine head speed of 0.3 in. min^{-1}, and fracture was instantly catastrophic from the original crack depth CO. Note that only a very small extent of SCG surrounding the initial crack appeared at a machine head speed of 0.2 in. min^{-1} (Fig. 7c).

3.4. Stress rupture observations

Thus far, it has been clearly demonstrated that SCG in hot-pressed Si_3N_4 (HS-130) starts at temperatures above 1200° C. To simulate practical applications, a few stress rupture tests were made to determine the extent of SCG when precracked specimens (constant initial crack size) were subjected at 1300° C to a fraction of the fracture stress (Fig. 8). Examination of the micrographs points out that when the magnitude of the applied stress is very large ($\geqslant 0.9\,\sigma_F$), fracture occurs very rapidly within a period of 0.5 min or less. However, even in such a short time, the SCG region had extended considerably compared to the specimen tested directly to failure (cf. Fig. 7a and 8a). At intermediate stress levels (around $0.75\,\sigma_F$), both the extent of SCG and time to failure increased substantially (Fig. 8b). Note that the growth of the initial crack in the depth direction (CO to DO) was much smaller than the growth along the edge, i.e. transverse (AB to EF). This presumably is due to the stress distribution in a bend specimen where the maximum stress in bending occurs along the outermost fibres on the tensile surface, i.e.

along edge EOF. At low stress levels, (around 0.5 to 0.6 σ_F), the extent of SCG decreased drastically while the time-to-failure increased as expected (Fig. 8c). In this case, the specimen did not break even after sustaining the stress for 40 min and, as such, was unloaded and broken at 20° C in order to reveal the extent of SCG. It appears that there exists a critical stress level below which no significant SCG occurs. To precisely define such a critical stress, long-term creep tests should be carried out.

4. Conclusions

(1) At room temperature, the fracture stress was dependent on crack length according to the Griffith criterion. Extrapolation of the data indicated that flaws of the order of 12 to 24 μm are responsible for brittle fracture of uncracked (virgin) material. The fracture surface energy, γ, measured at room temperature is about 22 000 erg cm^{-2}.

(2) The fracture stress for precracked specimens remained essentially constant from 20 to 1100° C, indicating the absence of crack tip blunting. Crack propagation in this temperature region is a combination of transcrystalline cleavage and intergranular fracture.

(3) The onset of significant subcritical crack growth (SCG) occurs at temperatures above 1200° C. The extent of SCG increases with increasing temperature and is entirely *intergranular* in nature. Catastrophic crack propagation subsequently occurs when the appropriate combination of crack length and stress level is achieved.

(4) The extent of subcritical crack growth at 1300° C decreased with increasing strain-rate and completely disappeared at high strain-rates.

(5) Preliminary stress-rupture tests indicate that significant subcritical crack growth does not occur at high temperatures below a critical stress level of about 0.5 σ_F.

Acknowledgements

This work was supported in part by the Advanced Research Projects Agency under contract DAAG 46-71-C0162 for which the authors would like to express their thanks.

References

1. R. J. LUMBY and R. F. COE, *Proc. Brit. Ceram. Soc.* **15** (1970) 91.
2. A. G. EVANS and J. V. SHARP, *J. Mater. Sci.* 6 (1971) 1292.
3. J. A. COPPOLA, R. C. BRADT, D. W. RICHERSON and R. A. ALLIEGRO, *Amer. Ceram. Soc. Bull.* **51** (1972) 847.
4. F. F. LANGE, *J. Amer. Ceram. Soc.* **56** (1973) 518.
5. R. KOSSOWSKY, *ibid* **56** (1973) 531.
6. D. W. RICHERSON, *Amer. Ceram. Soc. Bull.* **52** (1973) 560.
7. F. F. LANGE, *J. Amer. Ceram. Soc.* **57** (1974) 84.
8. S. D. HARTLINE, R. C. BRADT, D. W. RICHERSON and M. L. TORTI, *ibid* **57** (1974) 190.
9. A. G. EVANS and S. M. WIEDERHORN, *J. Mater. Sci.* **9** (1974) 270.
10. J. J. PETROVIC, L. A. JACOBSON, P. K. TALTY and A. K. VASUDEVAN, *J. Amer. Ceram. Soc.* **58** (1975) 113.
11. K. R. KINSMAN, R. K. GOVILA and P. BEARDMORE, in "Deformation of Ceramic Materials", edited by R. C. Bradt and R. E. Tressler (Plenum Press., New York, 1975) p. 465.
12. S. WILD, P. GRIEVESON and K. H. JACK, in "Special Ceramics V" edited by P. Popper, (The British Ceram. Res. Assoc., Stoke-On-Trent, 1972) p. 329.
13. H. F. PRIEST, F. C. BURNS, G. L. PRIEST and E. C. SKAAR, *J. Amer. Ceram. Soc.* **56** (1973) 395.
14. D. R. CLARKE and G. THOMAS, *ibid* **60** (1977) 491.
15. R. K. GOVILA, *Acta Met.* **20** (1972) 447.
16. P. KENNY, *Powder Met.* **14** (1971) 22.
17. N. INGELSTROM and H. NORDBERG, *Eng. Fract. Mech.* **6** (1974) 597.
18. K. R. KINSMAN, M. YESSIK, P. BEARDMORE and R. K. GOVILA, *Metallography* 8 (1975) 351.
19. A. A. GRIFFITH, *Phil. Trans. Roy. Soc.* **221** (1920) 163.
20. R. C. SHAH and A. S. KOBAYASHI, in "The Surface Crack: Physical Problems and Computational Solutions", edited by J. L. Swedlow (A.S.M.E., New York, 1972) p. 79.
21. A. F. McLEAN, E. A. FISHER and R. J. BRATTON, "Brittle Materials Design, High Temperature Gas Turbine", Tech. Rept. AMMRC CTR 74-26, April (1974).
22. J. J. PETROVIC, R. A. DIRKS, L. A. JACOBSON and M. G. MENDIRATTA, *J. Amer. Ceram. Soc.* **59** (1976) 177.
23. M. V. SWAIN, *J. Mater. Sci.* **11** (1976) 2345.
24. R. K. GOVILA and K. R. KINSMAN, *Amer. Ceram. Soc. Bull.* **57** (1978) 316.
25. J. J. PETROVIC and L. A. JACOBSON, in "Ceramics for High Performance Applications", edited by J. J. Burke, A. E. Gorum and R. N. Katz (Brook Hill, Mass., 1974) p. 397.
26. R. J. CHARLES, *J. Appl. Phys.* **29** (1958) 1657.
27. D. P. WILLIAMS and A. G. EVANS, *J. Test. and Eval.* **1** (1973) 264.
28. A. G. EVANS, L. R. RUSSELL and D. W. RICHERSON, *Met. Trans.* **6A** (1975) 707.

Received 20 June and accepted 6 September 1978.